

Thesis of the PhD dissertation

CAO TENG

BUDAPEST

2023



Hungarian University of Agriculture and Life Sciences

Faculty of Food Science

Department of Food Process Engineering

Doctoral (PhD)thesis

**CONTINUOUS AND CYCLIC PRODUCTION OF GALACTO-
OLIGOSACCHARIDES BY ULTRAFILTRATION-ASSISTED ENZYME
MEMBRANE REACTORS**

Cao Teng

Buda Campus

2023

The doctoral school:

Name: Doctoral School of Food Sciences

Discipline: Food Science

Head of doctoral school:


Livia Simonné Sarkadi, Professor, DSc
Hungarian University of Agriculture and Life Sciences,
Institute of Food Science and Technology

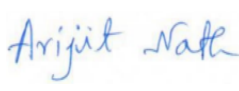
Supervisor(s):

Zoltán Kovács, Professor, PhD
Hungarian University of Agriculture and Life Sciences,
Institute of Food Science and Technology

Arijit Nath, University Research Associate, PhD
Hungarian University of Agriculture and Life Sciences,
Institute of Food Science and Technology

.....
Approval of the Head of Doctoral School


.....
Approval of the Supervisor
Zoltán Kovács


.....
Approval of the Supervisor
Arijit Nath

1. INTRODUCTION

Galacto-oligosaccharide (GOS) are non-digestible oligosaccharides, having 2–9 units of galactosyl residues with a terminal glucose linked by glycosidic linkages. They belong to prebiotic family and provide numerous health benefits. There has been evidence that it stimulates the immune system, improves intestinal motility, prevents intestinal infections, promotes calcium absorption and utilization, and displays anticancer and anti-obesity properties. Furthermore, GOS is confirmed as generally recognized as safe (GRAS) by the US Food and Drug Administration Agency (FDA) (Fijan, 2014, Kerry et al., 2018, Wan et al., 2019, Wilson and Whelan, 2017).

GOS is produced by trans-glycosylation reaction using β -galactosidase. The mechanism of GOS synthesis can be described by either thermodynamically controlled (the equilibrium of reaction towards glycosidic bond formation) or kinetically controlled (formation of glycosidic bond through activated glycosyl donor-enzyme donor complex) phenomena (de Albuquerque et al., 2021). β -galactosidase is producing by wide ranges of microorganisms, plants and animals. It has been reported that the characteristics of β -galactosidase depend on the source of organism and those impact the quality and quantity of the GOS yield, linkage type, and degree of polymerization (DP) (Gänzle, 2012, Torres et al., 2010).

Conventionally, GOS are mainly produced in batch procedures using soluble β -galactosidase in a stirred tank reactor (STR) in industry. This operation usually involves further enzyme inactivation and a complicated downstream enzyme removal process to obtain an enzyme-free saccharide mixture including GOS. The waste of expensive β -galactosidase and the high cost of enzyme removal process significantly contributes to the high price of GOS (Scott et al., 2016). Therefore, manufacturers of GOS are interested in finding a suitable technology where β -galactosidase can be reused. It may be believed that the use of ultrafiltration (UF)-assisted biocatalytic reactors, also known as enzymatic membrane reactors (UF-EMR) is a promising set-up with the aid of continuous synthesis of GOS and enzyme recovery.

EMR is typically consisted with a simple STR and an external UF membrane module. The membrane is dedicated to retain enzyme in reaction vessel, while saccharide fractions with lower

molecular weights pass through membrane pores. As a result, continuous synthesis of GOS and separation of enzyme in a simultaneous way can be achieved. Several studies have been carried out to investigate the performance of wide ranges of commercially available β -galactosidase for the synthesis of GOS in EMR. These β -galactosidase sources include yeast (*Kluyveromyces lactis*) (Pocedičová et al., 2010, Ren et al., 2015), fungus-*Aspergillus oryzae* (Córdova et al., 2016b, Matella et al., 2006), and bacterial (Das et al., 2011, Petzelbauer et al., 2002). Among them, β -galactosidase from *Bacillus circulans* is widely preferred by producers due to its superior thermal stability and able to offer high yield of GOS (Chen and Gänzle, 2017, Park and Oh, 2010, Warmerdam et al., 2014). The GOS yields (20%- 30%) obtained from EMR utilizing these enzymes were comparable to those obtained in STR under the same operation conditions. The majority of experiments were conducted under short-time (<5h) and laboratory-scale (<4L) set-up.

There are limited information about the performance of *Bacillus circulans* enzymes for GOS production in EMR setups. Warmerdam et al. reported a commercial available enzyme, Biolacta N5 from *Bacillus circulans*, has half-lives of 29h, 29h, and 16 h at 25°C, 40°C, and 60°C, respectively, under 30 % w·w⁻¹ initial lactose concentration in STR (Warmerdam et al., 2013). Authors also reported that the enzyme has greater stability at higher lactose concentrations. Limited numbers of investigations addressed the stability of β -galactosidase over prolonged biocatalysts process, ranging from 100 to 200 hours. It was reported that there was no significant loss of the activity of β -galactosidase after 96 h (Ren et al., 2015). Moreover, other investigators reported that half-life of a heat tolerant β -galactosidase is approximately 7 days (Petzelbauer et al., 2002). These observations of enzyme stability suggest that for GOS production, the free enzyme EMR process has great potential.

The research objective of this study was to investigate the performance of commercially available β -galactosidase from *Bacillus circulans* (Biolacta N5) in UF-EMR setup to produce GOS in a continuous and batch manner. Efforts have been placed to find out superior operational strategy of EMR to obtained high yield of GOS and enzyme recovery. Furthermore, the stability of enzyme during biocatalytic reaction in different operational mode has also been investigated.

2. OBJECTIVES TO ACHIEVE

The main objective of this investigation was to understand the performance of commercially available Biolacta N5 for the synthesis of GOS by ultrafiltration-assisted enzyme membrane reactors (UF-EMR). In order to achieve this aim, a research methodology including both theoretical and experimental investigations have been designed, mentioned below.

1. In-silico studies were carried out to predict the formation of enzyme-free GOS by EMR, operated with continuous mode. Kinetic equations dedicated to biocatalytic reactions and enzyme stability reported in peer-reviewed literature were adopted for simulation purposes. Subsequently, a mathematical framework was developed to describe GOS formation by EMR, operated with continuous mode. Simulation studies were performed by using numerical software packages.
2. An ultrafiltration-assisted membrane reactor (UF-EMR) utilizing free β -galactosidase was developed. It was designed and equipped with necessary control system to operate at a constant product flow. The performance of this EMR was used in experiment, more specifically,
 - a) Preliminary filtration tests with the reaction liquor were performed to characterize the flux behavior of the UF membrane.
 - b) The dependence of transmembrane pressure (TMP) and enzyme load in biocatalytic reaction on the permeate flux was experimentally determined.
 - c) A membrane cleaning procedure was proposed, and its efficiency for regenerating the membrane was evaluated.
 - d) A series of short-term experiments were conducted by operating the EMR in continuous fashion, typically for 6–9 h. These tests were performed to determine the steady-state performance of the EMR in terms of yield and productivity. The effect of residence time and enzyme load on the biocatalytic reaction was investigated under fixed operational parameters, such as temperature, pH of reaction medium, concentration of lactose in feed

and recirculation flowrate.

- e) The catalytic performance of the continuous-EMR was investigated for an extended period of time (over 120 h).

3. A three-step procedure with five cycles for the production of GOS in cyclic-EMR was designed. A comparative analysis between the performance of cyclic-EMR and traditional STR was performed. In the scope of this study, the following tasks were considered.

- a) A series of batch mode investigations were performed with STR. Different known initial concentration of enzyme was considered in biocatalytic reaction. The relationship between the experimental reaction rate and the applied enzyme dose was explored by analyzing the concentration of the individual saccharide over time. Initial reaction rate and enzyme activity were used to understand the correlation among them, and the results were used for calibration purposes.
- b) Once the initial reaction velocity of each saccharide fraction in cyclic-EMR was determined from the progress curve, the loss of enzyme activity in successive cycles was estimated by using determined correlation and the results from STR.

3. MATERIALS AND METHODS

3.1. Materials

All experiments utilized Biolacta N5 (Amano Enzyme Inc., Nagoya, Japan), a β -galactosidase derived from *Bacillus circulans*, as a catalyst to convert lactose into GOS. Except for the long-term experiments, Lactochem Fine Powder, a pharmaceutical-grade α -lactose monohydrate provided by FrieslandCampina Domo B. V. (Amersfoort, The Netherlands), was utilized as the substrate in all tests. Lactopure Regular Power 150 M (FrieslandCampina Domo B.V., Amersfoort, The Netherlands), a food-grade lactose preparation derived from whey with a typical lactose content of 99.7%, was used for the long-term campaigns (see Sect. 3.5.4).

3.2. Enzyme activity assay

A direct measurement method was used to measure the activity of Biolacta N5 using $300 \text{ g} \cdot \text{kg}^{-1}$ lactose as substrate. Deionized water was served as a reaction buffer, and NaOH was added in order to adjust the pH to 6.0. Biolacta N5 at a concentration of $0.91 \text{ g} \cdot \text{kg}^{-1}$ was added to the reaction solution to commence the reaction. Three replications were performed for the reaction. Upon completion of a 20-minute incubation at 50°C , the reaction was further heated for 30 minutes at 90°C to terminate the reaction. The concentration of DP2 was determined by High Performance Liquid Chromatography (HPLC) as described in Sect. 3.8. Under the specified reaction conditions, one unit of enzyme activity (U) was defined as the amount of enzyme needed to transform (or converted) $1 \mu\text{mol}$ of DP2 per minute.

3.3. Modelling transgalactosylation reactions

In-silico studies were carried out to predict the performance of STRs and continuous-EMRs in producing GOS. First, selected kinetic models (see Eq. 3.3-1 – Eq. 3.3-6) and enzyme stability models (see Eq. 3.3-12) reported in literature were adopted for simulation purposes of STR performance. Then, a mathematical framework was developed for describing GOS conversion in continuous-EMRs. Simulation studies were performed by using Scilab (version 6.1.1, 2021), a numerical software package by Scilab Enterprises (France). Model simulations were carried out

by the numerical integration of sets of ordinary differential equations (ODEs) using the function *ode*, the built-in ODE solver of Scilab.

The four-step kinetic model by Palai et al.,(2012) can be represented by the following set of ordinary differential equations:

$$\frac{d[E]}{dt} = -k_1[E][L] + k_{-1}[EL] + k_3[EM][L] - k_{-3}[E][G] + k_4[EM][G] \quad \text{Eq. 3.3-1}$$

$$\frac{d[EL]}{dt} = k_1[E][L] - k_{-1}[EL] - k_2[EL] \quad \text{Eq. 3.3-2}$$

$$\frac{d[EM]}{dt} = k_2[E][L] - k_3[EM][L] + k_{-3}[E][G] - k_4[EM][G] \quad \text{Eq. 3.3-3}$$

$$\frac{d[L]}{dt} = -k_1[E][L] + k_{-1}[EL] - k_3[EM][L] + k_{-3}[E][G] \quad \text{Eq. 3.3-4}$$

$$\frac{d[M]}{dt} = k_2[EL] \quad \text{Eq. 3.3-5}$$

$$\frac{d[G]}{dt} = k_3[EM][L] - k_{-3}[E][G] \quad \text{Eq. 3.3-6}$$

where E, M, L and G denote enzyme, monosaccharides (glucose and galactose), lactose and GOS (DP>3) respectively and k values are the rate constants for step reactions.

The two-stage series mechanism of inactivation is represented by the scheme:



where E_0 , E_1 , and E_2 represent the enzyme activity at initial, intermediate, and final state, respectively, k_1 and k_2 are the deactivation velocity coefficients, and α_1 and α_2 are the ratio of specific activities of E_1/E_0 and E_2/E_0 , respectively.

The relative enzyme activity y at specific time t can be calculated as:

$$y = \left[1 + \frac{\alpha_1 k_1 - \alpha_2 k_2}{k_2 - k_1} \right] \exp(-k_1 t) - \left[\frac{\alpha_1 k_1 - \alpha_2 k_2}{k_2 - k_1} \right] \exp(-k_2 t) + \alpha_2, \quad \text{Eq. 3.3-8}$$

If the enzyme is assumed to be completely inactivated at its final state, i.e., $\alpha_2=0$, then Eq. 3.3-2 is reduced to

$$y = \left[1 + \frac{\alpha_1 k_1}{k_2 - k_1} \right] \exp(-k_1 t) - \left[\frac{\alpha_1 k_1}{k_2 - k_1} \right] \exp(-k_2 t) \quad \text{Eq. 3.3-9}$$

A specific case of the above model is the single-step model with non-zero activity at the final

enzyme state, such that $k_2=0$. In this case, the reaction scheme is reduced to:



and Eq.3.3-9 can be simplified to:

$$y = (1 - \alpha_1) \exp(-k_1 t) + \alpha_1, \quad \text{Eq. 3.3-5}$$

If the native (active) enzyme is assumed to be converted in a one-step reaction into an inactive structure, i.e., $\alpha_1 = 0$, then the model can be further reduced to:

$$y = \exp(-k_1 t), \quad \text{Eq. 3.3-12}$$

This latter, simplified model is known as the single-step first-order model.

3.4. Stirred tank reactor (STR)

3.4.1. Enzymatic conversion in batch fashion

Using the batch stirred tank reactor (STR), small-scale batch experiments were conducted with enzyme activities ranging from 923 to 92301 U·kg⁻¹ to determine whether enzyme load has a significant effect on reaction rate. In each test, a reaction solution consisting of 300 g·kg⁻¹ lactose was prepared in a beaker and placed on hotplate magnetic stirrer for 24-48 h under the reaction conditions of temperature 50 °C and pH 6.0 at 60 rpm throughout the operation. Prior to HPLC analysis, samples were collected at periodic intervals (5min, 30min, and/or 1h) and inactivated at 90 °C for 30 minutes.

3.4.2. Evaluation of process curves

According to the model adopted from Pázmándi et al.,(2018), the progression curves of individual saccharides fractions in STR were evaluated at different enzyme loads (from 0.1 g·kg⁻¹ to 10 g·kg⁻¹). The saturation model describes the concentration of the generated saccharides fractions (e.g., glucose, galactose, and GOS fractions) in relation to incubation time:

$$F(t) = C_0 + p_1(1 - e^{-p_2 t}) \quad \text{Eq. 3.4.2-1}$$

where t was the reaction time, C_0 was the initial concentration of saccharides, and $p_1 \times p_2$ was the

initial reaction velocity (i.e., slope of the curve at time point $t = 0$). While $p_2 > 0$, in case of DP2 (expressed in $\text{g} \cdot \text{kg}^{-1}$), $p_1 < 0$ (F was decreasing), in all other cases $p_1 > 0$ (F was increasing).

As a next step, a linear function with no intercept was fitted to the enzyme activity of various saccharide fractions (presented by saccharide concentrations) in relation to their initial reaction velocities ($p_1 \times p_2$). The normality of the model residuals was checked by their skewness and kurtosis (the absolute values were all below 1). An ANOVA F-test was conducted to determine the accuracy of the model. Additionally, t-tests were performed on the parameter estimations. Finally, the explained variance rates (R^2) were computed, and their significance was evaluated. The statistical assessment was performed with the statistical software IBM SPSS v27 (Armonk, NY) (IBM Corp. Released 2017. IBM SPSS Statistics for Windows).

3.5. Continuous enzyme membrane reactor (Continuous-EMR)

3.5.1. Construction of continuous EMR

An overview of the flowsheet for the (semi-) pilot scale EMR used in the continuous production of GOS can be seen in Figure 1.

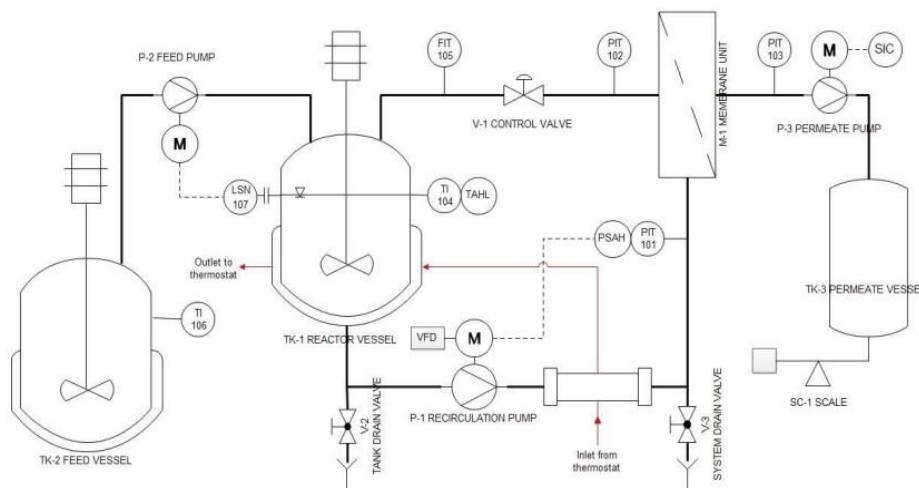


Figure 1. Piping and instrumentation diagram of continuous ultrafiltration-assisted enzymatic reactor (EMR).

It consists of two components: a stirred-tank reactor (TK-1) and an external ultrafiltration module (M-1). The 10 kDa UF membrane with a filtration area of approx. 0.37 m^2 was made of a

polyethersulfone active layer cast on polypropylene backing material. Through this set-up, it was possible to control the recirculation flow rate, the retentate pressure, the temperature, the permeate flow, and the liquid level in TK-1 during operation.

3.5.2. Preliminary filtration tests

In order to narrow the operating conditions of the filtration process, two preliminary tests were performed. The tests were performed in a total-recycle mode, in which both retentate and permeate streams were recycled back into the reactor. The recirculation flowrate of the retentate was set to $0.18 \text{ m}^3 \cdot \text{h}^{-1}$. The experiments were performed with 2 kg of process liquid consisting of 30% w·w⁻¹ lactose under the condition of pH 6.0 and temperature at 50 °C. The permeate flux was monitored during the test runs to investigate the filtration performance of the UF membrane. Chemical analysis of the samples was not conducted.

3.5.3. Short-term enzymatic conversion

An EMR was operated continuously for eight short-term tests (typically for 6 to 9 hours) using a 30 w·w⁻¹% lactose solution at pH 6.0 and 50°C. The experiments were performed by varying the enzyme load (between 923 to 92301 U·kg⁻¹) and the permeate flow (between 0.8 and 1.8 kg·h⁻¹) under otherwise identical conditions. There was a two-kilogram solution of lactose added to the reactor, and the remaining solution was stored in a thermostatic substrate tank. Once a certain amount of Biolacta N5 dosage (from 23 to 92301 U·kg⁻¹) has been administered, the circulation pump has been operated at a crossflow rate of $0.17 \pm 0.01 \text{ m}^3 \cdot \text{h}^{-1}$. A pressure-adjusting valve was used to set a retentate pressure of 0.5 bar. A constant permeate flow rate was achieved by adjusting the rotational speed of the permeate pump. This resulted in a constant residence time for the permeate. A constant volume in the reactor was maintained by continuously adding 300 g·kg⁻¹ fresh substrate solution and removing the enzyme-free product at the same rate during the entire process. In order to analyze the carbohydrate content of the permeate stream, samples were taken periodically. The membrane was cleaned in accordance with the procedure described in Sect.3.7.

3.5.4. Long-term enzymatic conversion

Two long-term experiments, designated L1 and L2, were conducted under identical operating conditions for an extended period of time (over 100 hours). In both runs, the operation was conducted by dosing 46151 U·kg⁻¹ (10 g of crude enzyme) of Biolacta N5 in 2 kg of reaction liquid with 30 w·w⁻¹% lactose concentration at 50 °C and pH 6.0. The retentate pressure was adjusted to 1.0 bar in both runs. The permeate pump was set to generate a constant flowrate of 1.1 kg·h⁻¹, resulting in a residence time of 1.8 h. The recirculation flowrate was set to 0.17 m³·h⁻¹. HPLC analysis was conducted on three samples taken from the permeate stream during each periodic sampling. Analyses of samples taken from L1 were conducted by HPLC without pretreatment. The deactivation of three samples in L2 was accomplished by heat deactivation (90 °C, 30 min), acid deactivation (HCl), and analysis without deactivation pretreatment. Membrane cleaning was performed as described in Sect. 3.7.

3.5.5. Performance assessment

Nonlinear regression was employed to evaluate the relationship between the steady-state carbohydrate composition and the operational factor ($\tau \times c_E$). An arbitrary selected empirical model was fitted to the experimental measurements of the reaction products, including DP3-6, glucose, and galactose, as a function of operational parameters to derive the following quantitative relationship:

$$w_i = \frac{b_1 c_E \tau}{b_2 c_E \tau + 1} + \varepsilon \quad \text{Eq. 3.5.5-1}$$

where w_i represents the relative mass percentage of the individual saccharide fraction at steady state, b_1 and b_2 stand for the model coefficients, τ was the residence time, c_E indicates the enzyme concentration, and ε was the error term. This regression model was used for the DP2 fraction as follows:

$$w_{DP2} = 100 - \frac{b_1 c_E \tau}{b_2 c_E \tau + 1} + \varepsilon \quad \text{Eq. 3.5.5-2}$$

The statistical assessment was carried out using the statistics and curve fitting toolboxes

implemented in (MATLAB, R2015a) (The Mathwork Inc., Natick, MA, USA).

3.6. Cyclic enzyme membrane reactor (Cyclic-EMR)

3.6.1. Construction of cyclic-EMR

With the lab-scale equipment shown in Figure 2, the production of GOS was carried out batchwise, over a number of cycles. A stirred tank reactor (STR) and an exterior ultrafiltration membrane unit (UF) were the main components of the cyclic enzyme membrane reactor (cyclic-EMR). A polyethersulfone hollow-fiber module (type: FB02-CC-FUS-0382) of 0.26 m² and 30 kDa was included in the membrane unit (M1).

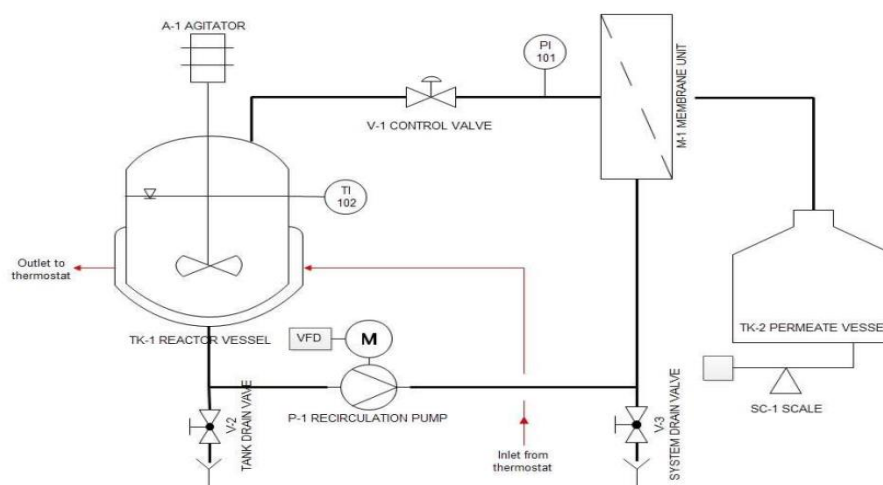


Figure 2. Piping and instrumentation diagram of cyclic -EMR.

3.6.2. Enzymatic conversion in cyclic-EMR

A protocol consisting of three operational steps in five successive cycles was used to carry out the enzymatic conversion:

1. In the first step, a traditional STR, TK-1, was employed to carry out a batchwise reaction. The reaction was initiated by dosing an initial enzyme activity of 8307 U·kg⁻¹ (0.9 g·kg⁻¹) to 9.5 kg reaction solution with an initial lactose concentration of 300 g·kg⁻¹ at 50 °C and pH 6.0. Periodic samples were taken from the reactor and heat-treated at 90 °C for 30 minutes prior to the measurement of saccharides by HPLC.

2. Following the first step, the membrane unit M-1 was attached to the reactor, and the reaction liquid was filtered through UF at 0.5 bar transmembrane pressure until 8.4 kg of permeate was collected.
3. A third step involved the de-attachment of the membrane module M-1 from the plant. 8.4 kg of fresh substrate solution consisting of $300 \text{ g}\cdot\text{kg}^{-1}$ of lactose was added to the concentrated enzyme solution in the reactor to maintain a constant volume in TK-1. Afterward, step 1 of the next cycle was initiated. After the membrane was de-attached, it was cleaned in accordance with Sect.3.7.

3.6.3. *Performance assessment*

The saturation model described in Sect. 3.4.2 was used to verify the concentration of the generated saccharide fractions (e.g., glucose, galactose and GOS fractions) in relation to the reaction time. The two-stage series mechanism (Torres and Batista-Viera, 2012, Urrutia et al., 2013, Vera et al., 2011) and its simplified forms (Albayrak and Yang, 2002, Huang et al., 2020, Warmerdam et al., 2013) were used to quantify the stability of lactose-converting β -galactosidase over time.

3.7. **Membrane regeneration**

Deionized water was tested for permeability prior to each test with the process liquor. Upon completion of each filtration step, the membrane was cleaned in four steps as follows:

1. A NaOH solution ($\text{pH} = 10\text{-}11$) was circulated for 1-2 hours at $40\text{-}50 \text{ }^{\circ}\text{C}$ under 0.5-1 bar pressure for the purpose of cleaning the membrane.
2. For the removal of the cleaning agent, the plant was drained and flushed with water several times.
3. The permeability of the cleaned membrane was determined using DI water. Occasionally, when the original membrane permeability was recovered less than 75% by alkaline cleaning, subsequent cleaning with citric acid and/or Ultrasil 10 (sodium based alkaline EDTA) membrane cleanser (Ecolab, Paul, MN, USA) has been performed ($1 \text{ w}\cdot\text{w}^{-1}\%$, $40\text{-}50 \text{ }^{\circ}\text{C}$, 0.5^{-1}

bar, 0.5⁻¹ h).

4. During overnight storage, the module was immersed in a saturated salt solution to prevent microbial growth and membrane drying out.

3.8. HPLC

In accordance with the methodology described in (Pázmándi et al., 2018), carbohydrate compositions of samples (glucose, galactose, and DP2-6 fractions) were determined by high performance liquid chromatography (HPLC). There were three main components to the HPLC system, including (1) Thermo Separation, which includes an Intersciences SCM1000 degasser, a gradient pump P200, a built-in column oven, and an Autosampler AS100; (2) a Shodex R-101 refractive index detector from Showa Denko Europe GmbH, Munich, Germany; and (3) an N2000 Chromatography Data System from Science Technology (Hangzhou) Inc. (Hangzhou, China). Chromatography Data System N2000 performs peak detection and integration. The RNM carbohydrate 8 % Na+ 300 × 7.8 (Phenomenex, Torrance, CA, USA) analytical column and a guard column were used under the condition of 50 °C at 0.2 mL·min⁻¹ with a mobile phase of pre-filtered (2 µm) DI water.

3.9. HPLC

In this investigation, the following measures were employed:

Relative mass percentage fraction (w_i) was calculated as the ratio of the mass of a saccharide fraction i (m_i) to the total mass of saccharides present in the solution:

$$w_i = \frac{m_i}{\sum m_i} \times 100\% \quad \text{Eq. 3.9-1}$$

Residence time (τ) was determined by the weight of the reaction liquor in the reactor (V) dividing the mass flow rate of the permeate (q):

$$\tau = \frac{V}{q} \quad \text{Eq. 3.9-2}$$

Yield (Y) in percentage was defined as the concentration of the synthesized GOS (DP3-6) fractions (C_{DP3-6}) divided by the concentration of lactose in the feed (C_L):

$$Y = \frac{c_{DP3-6}}{c_L} \times 100\%$$

Eq. 3.9-3

Biocatalyst productivity (P) was defined as the total quantity of DP3-6 formed by one unit of crude enzyme preparation per hour:

$$P = \frac{c_{DP3-6}}{c_{ET}}$$

Eq. 3.9-4

4. RESULTS AND DISCUSSION

4.1. Modelling transgalactosylation reactions

The main objective of the modeling study reported in this section was to simulate the performance of continuous-EMRs utilizing free enzymes and to predict the system behavior as a function of main operational parameters such as enzyme load and residence time.

4.1.1. Kinetic model development

The mathematical kinetic model describing enzyme kinetics on GOS synthesis proposed by Palai-model (Palai et al., 2012) was selected for further mathematical analysis.

The simulation results by using a numerical software package suggest that a gradual decrease in lactose concentration occurs in the solution over time. It was to note that the concentration of GOS increases continuously after the start of the reaction until reaching a maximum of approx. 35% $w \cdot w^{-1}$. After that, the concentration of GOS tends to decrease. The time of reaching GOS peak was greatly influenced by the actual enzyme load. The concentration of monosaccharides in the solution consistently increases over time. It was, however, obvious from the simulation results that a careful selection of enzyme load and incubation time was required in order to terminate the reaction at maximum GOS yield.

According to the simulated model, the β -galactosidase was present in three forms, including the non-reacted enzyme, the enzyme-lactose complex, and the enzyme-monosaccharide complex. The results indicated that within a short time after the reaction begins, the enzyme forms enzyme-sugar complexes with e.g., lactose and monosaccharides. There was a predominance of enzyme-monosaccharide complexes in the mixture (approx. 99%), while uncatalyzed enzymes and enzyme-lactose complexes constitute a small percentage of the total enzymes and can be neglected.

4.1.2. Performance simulation of continuous-EMRs

It is important to note that previous modeling studies considered batch synthesis of GOS in STRs. The scope of my experimental investigations was, however, continuous GOS synthesis in EMRs.

In this section, I report the mathematical problem formulation for EMR set-ups and perform simulations under ideal conditions, i.e., assuming no activity losses during EMR runs.

For the performance assessment, I consider continuous GOS synthesis carried out by an EMR utilizing soluble Biolacta N5. In continuous-EMR, the fresh substrate with a lactose concentration of L_f was continuously supplied into the reactor, and the enzyme-free product stream was continuously removed. The volumetric flow rate of the feed (q_{in}) was equal to that of the permeate (q_{out}), thus the volume of the reaction liquid (V) in the EMR was kept constant. The residence time was then given as $\tau = V/q$.

Assuming a well-mixed state in the reactor, the general mass balancing equation for component i can be written as:

$$\frac{d[m_i]}{dt} = q_{in}[C_{i,in}] - q_{out}[C_{i,out}] + V[R_i] = \frac{V}{\tau}[[C_{i,in}] - [C_{i,out}] + V[R_i]] \quad Eq.4.1.2-1$$

where m_i , C_i , and R_i were the mass, the concentration, and the production rate of component i in the reaction vessel, respectively.

Given that $q_{in}=q_{out}=q$ and $q = V/\tau$, the following differential equations can be derived for the individual saccharide fractions.

Component balance describing the change in lactose concentration in the EMR:

$$\frac{d[L]}{dt} = \frac{V}{\tau} ([L_f] - [L]) + V[R_L] \quad Eq.4.1.2-2$$

where L and L_f were the concentration of lactose in the permeate stream and feed respectively.

Component balance for monosaccharides, given that the monosaccharides concentration in the feed was zero:

$$\frac{d[M]}{dt} = -\frac{V}{\tau} [M] + V[R_M] \quad Eq.4.1.2-3$$

Component balance for GOS, the feed GOS concentration equals to zero, then:

$$\frac{d[G]}{dt} = -\frac{V}{\tau} [G] + V[R_G] \quad Eq.4.1.2-4$$

Integrating the enzyme kinetics model proposed by Palai et al. (2012) into our mathematical framework, the following initial value problem can be defined:

$$\frac{d[E]}{dt} = -k_1[E][L] + k_{-1}[EL] + k_3[EM][L] - k_{-3}[E][G] + k_4[EM][G] \quad \text{Eq.4.1.2-5}$$

$$\frac{d[EL]}{dt} = k_1[E][L] - k_{-1}[EL] \quad \text{Eq.4.1.2-6}$$

$$\frac{d[EM]}{dt} = k_2[EL] - k_3[EM][L] + k_{-3}[E][G] - k_4[EM][G] \quad \text{Eq.4.1.2-7}$$

$$\frac{d[L]}{dt} = -k_1[E][L] + k_{-1}[EL] - k_3[EM][L] + k_{-3}[E][G] + \frac{V}{\tau}([L_F] - [L]) \quad \text{Eq.4.1.2-8}$$

$$\frac{d[M]}{dt} = k_2[EL] - \frac{V}{\tau}[M] \quad \text{Eq.4.1.2-9}$$

$$\frac{d[G]}{dt} = k_3[EM][L] - k_{-3}[E][G] - \frac{V}{\tau}[G] \quad \text{Eq.4.1.2-10}$$

where $[E]$, $[E_1]$, $[M]$, $[L]$ and $[G]$ denote the concentration of enzyme, inactive enzyme in the retention side, and monosaccharides (glucose and galactose), lactose and GOS ($DP_{3\geq}$) in the permeate given in $M \cdot L^{-1}$, respectively. The k values represent the reaction rate constants showed in previous literature by Palai et al., (2012).

The above reported set of ordinary differential equations (ODEs) were then employed to describe the formation and transformation of individual carbohydrate compounds in the EMR.

The initial value problem represented in (Eq.4.1.2-5-Eq.4.1.2-10) with the model parameter values was implemented in Scilab, and the dynamic behavior of the EMR system was simulated. More specifically, I investigated the time-course of the concentration of the individual saccharide compounds for varying the residence time (up to 10h) and the enzyme activity (up to $92301 \text{ U} \cdot \text{kg}^{-1}$, i.e., up to an enzyme load of $10 \text{ g} \cdot \text{L}^{-1}$). The scenario analysis was performed at fixed reaction conditions of $320 \text{ g} \cdot \text{L}^{-1}$ lactose concentration, pH 6.0, and 40°C .

The steady state was typically reached after about one hour of process run. Under the given operational settings, by increasing enzyme activity from $923 \text{ U} \cdot \text{kg}^{-1}$ to $92301 \text{ U} \cdot \text{kg}^{-1}$, lactose conversion increases from $18\% \text{ w} \cdot \text{w}^{-1}$ to approximately $42\% \text{ w} \cdot \text{w}^{-1}$, whereas GOS yield increases by approximately $5\% \text{ w} \cdot \text{w}^{-1}$ (from $13\% \text{ w} \cdot \text{w}^{-1}$ to $28\% \text{ w} \cdot \text{w}^{-1}$).

The interrelated effect of residence time and enzyme activity on GOS synthesis can be expressed by using a combined operational parameter, $\tau \times c_E$, which was the product of residence time (τ)

and enzyme load (c_E). Figure 3 depicts the variation of GOS, monosaccharides, and DP2 concentrations as a function of $\tau \times c_E$.

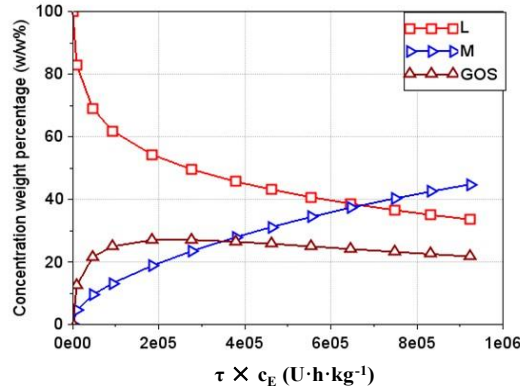


Figure 3. Steady-state composition saccharides as function of $\tau \times c_E$ (U·h·kg⁻¹). \square : DP2, Δ : GOS, \triangleright : Monosaccharides (glucose and galactose).

It is important to highlight that GOS yield peaks at a certain value of $\tau \times c_E$. According to my simulation results, in the continuous-EMR, the maximal GOS production (28% w·w⁻¹) was obtained by adjusting the product of residence time and enzyme activity to a value of approx. 180,000 U·kg⁻¹. As depicted in Figure 3, a distinct characteristic of the examined reactor configuration is that beyond a certain threshold value of $\tau \times c_E$, the GOS yield ceases to increase.

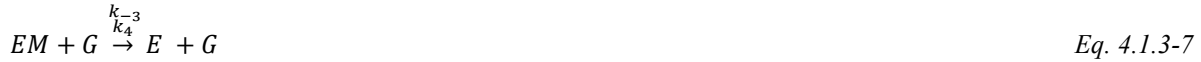
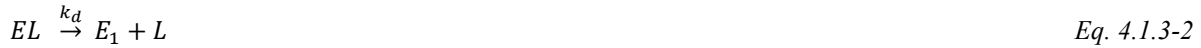
My results indicate that concentrations of GOS were in the range of 0-28% w·w⁻¹ depending on the settings of operational parameters. It is noteworthy that this yield was less than the maximum GOS yield (35% w·w⁻¹) obtained in biocatalytic reactions in STR under the same reaction conditions. There was an overall trend for an increase in GOS concentration with an increase in residence time and enzyme activity. Accordingly, I was to determine the optimal range of operating parameters for achieving maximum GOS yield in continuous-EMR.

4.1.3. Accounting for enzyme activity losses

It is important to note that all mathematical models reported in the open literature, that deal with the kinetics of GOS synthesis, ignore enzyme inactivation. However, previous experimental research by Warmerdam et al. (2013) has demonstrated that, in the batch STR enzyme catalysis process, a considerable enzyme inactivation occurs. According to their research, a first-order

enzyme inactivation model provides an adequate explanation for the degradation of Biolacta N5 over time. Biolacta N5 has been determined to have half-lives of 29, 29 and 16 hours at 25°C, 40°C, and 60°C, respectively, at a 30% w·w⁻¹ initial lactose concentration. Warmerdam and her coworkers considered 4 forms of the enzyme during the reaction, which include unreacted enzyme, enzyme-lactose complex, enzyme-monosaccharide complex, and inactivated enzyme. To be more precise, the first three forms of enzyme undergo varying degrees of inactivation over time. According to Palai et al.,(2012), the predominant enzyme-monosaccharide compound will also play a significant role in enzyme inactivation.

The inactivation model proposed by Warmerdam et al. (2013) can be integrated into our mathematical framework presented in Eq.4.1.2-5 to Eq.4.1.2-10. Thus, the extended reaction scheme, that accounts also for activity losses during the continuous-EMR process, reads as:



Then, a set of ordinary differential equations (ODEs) that describe the performance of the EMR were given as:

$$\frac{d[E]}{dt} = -k_1[E][L] + k_{-1}[EL] + k_3[EM][L] - k_{-3}[E][G] + k_4[EM][G] - k_d[E] \quad \text{Eq. 4.1.3-8}$$

$$\frac{d[E_1]}{dt} = k_d[E] + k_d[EL] + k_d[EM] \quad \text{Eq. 4.1.3-9}$$

$$\frac{d[EL]}{dt} = k_1[E][L] - k_{-1}[E] - k_d[EL] \quad \text{Eq. 4.1.3-10}$$

$$\frac{d[EM]}{dt} = k_2[EL] - k_3[EM][L] + k_{-3}[E][G] - k_4[EM][G] - k_d[EM] \quad \text{Eq. 4.1.3-11}$$

$$\frac{d[L]}{dt} = -k_1[E][L] + k_{-1}[EL] - k_3[EM][L] + k_{-3}[E][G] + \frac{V}{\tau}([L_F] - [L]) + k_d[EL] \quad \text{Eq. 4.1.3-12}$$

$$\frac{d[M]}{dt} = k_2[EL] - \frac{V}{\tau}[M] + k_d[EM] \quad \text{Eq. 4.1.3-13}$$

$$\frac{d[G]}{dt} = k_3[EM][L] - k_{-3}[E][G] - \frac{V}{\tau}[G] \quad \text{Eq. 4.1.3-14}$$

where $[E]$, $[E_1]$, $[M]$, $[L]$ and $[G]$ denote the concentration of enzyme, inactive enzyme in the retention side, and monosaccharides (glucose and galactose), lactose and GOS (DP3 \geq) in the permeate given in $\text{M}\cdot\text{L}^{-1}$, respectively. The k values represent the reaction rate constants, and k_d was the enzyme inactivation constant in h^{-1} . The estimated values of parameters were adopted from literature (Warmerdam et al., 2013).

I conducted a series of simulation trials under various enzyme activities (up to $10^5 \text{ U}\cdot\text{h}\cdot\text{kg}^{-1}$, i.e. $10 \text{ g}\cdot\text{L}^{-1}$) and residence times (ranging from 0 to 10 h). Eq.4.1.3-8-Eq.4.1.3-14 were employed to determine the concentration of different carbohydrates as a function of time in the biocatalytic reaction process.

The results show that in a typical short-term (4-hour) EMR run under fix operational settings of $320 \text{ g}\cdot\text{L}^{-1}$ initial lactose concentration, $10 \text{ g}\cdot\text{L}^{-1}$ enzyme load, 2.2 h residence time, pH 6.0, and 40°C . Lactose was converted into monosaccharides and GOS, reaching a maximum lactose conversion of approximately 42% $\text{w}\cdot\text{w}^{-1}$ after two hours. Meanwhile, the concentrations of monosaccharides and GOS also reached maximum of 28% $\text{w}\cdot\text{w}^{-1}$. Note that the maximum GOS concentration achieved in continuous-EMR (28% $\text{w}\cdot\text{w}^{-1}$) was lower than that of STR (35% $\text{w}\cdot\text{w}^{-1}$) under the same reaction conditions (initial lactose concentration $320 \text{ g}\cdot\text{L}^{-1}$, $10 \text{ g}\cdot\text{L}^{-1}$ Biolacta N5 load, pH 6.0, 40°C).

However, for the system behavior predicted by the model for a long-term run (400 h). As enzyme activity declines over time, the GOS catalysis deteriorates. At the stage of complete inactivation, the lactose concentration in the permeate was the same as in the feed. Also, the concentration of GOS eventually decreases to zero.

According to my simulations, within a short time after starting the reaction, the active enzyme rapidly binds to the substrate and releases the monosaccharide. The enzyme binds to the monosaccharide to form an enzyme-monosaccharide complex. Within a short time, the majority of the enzyme in solution exists as an enzyme-monosaccharide complex and the concentration

increases rapidly. The enzyme activity gradually decreases with time and ultimately becomes completely inactive. When the enzyme was completely inactivated, the concentration of the enzyme-monosaccharide complex in the reaction solution was zero at this time.

4.1.4. Enzyme inactivation model development

Within the scope of my modeling study, I conducted a systematic literature review (reported in Sect. 3.9) and identified a number of models applicable to describing the transgalactosylation reaction catalyzed by β -galactosidase from a *Bacillus circulans* source. These include the model describing the kinetics of transgalactosylation proposed by Palai et al. (2012) and the model of enzyme inactivation proposed by Warmerdam et al (2013). I successfully replicated their reported results in STR and confirmed their validity. Then, I have developed a mathematical framework for describing GOS synthesis in EMR without and with enzyme inactivation.

I found that, under ideal conditions of no enzyme inactivation, the predicted steady-state GOS yield in the EMR ($\sim 30\% \text{ w}\cdot\text{w}^{-1}$) was slightly lower than the maximum yield in the STR ($\sim 34\% \text{ w}\cdot\text{w}^{-1}$) under optimal reaction conditions. When enzyme inactivation was considered, the GOS concentration in the EMR decreases over time and eventually reaches zero. My simulation results suggest that the activity of the enzyme during EMR runs must be strictly monitored. In order to maintain a stable GOS yield in the product stream, different control strategies can be applied, such as an increase in the residence time or the addition of fresh enzymes to compensate for the loss of enzyme activity.

4.2. Stirred-tank reactor (STR)

Eight lab-scale (typically 0.1-0.3 L) batch experiments were carried out using Biolacta N5 from *Bacillus circulans*. The enzyme concentration on GOS yield was investigated under the reaction conditions of an initial lactose concentration of $300 \text{ g}\cdot\text{kg}^{-1}$, temperature of 50°C , and pH 6.0. The reaction was carried out for an operation time of 24h.

The results showed that, within the enzyme activity range from $923 \text{ U}\cdot\text{kg}^{-1}$ to $92301 \text{ U}\cdot\text{kg}^{-1}$, all experiments showed the same tendency, i.e., the GOS concentration increasing up to a maximum

of approx. 38% on the basis of total carbohydrates then it decreases. In the case of enzyme activities in the range 923-9230 U·kg⁻¹, the galactose production from the hydrolysis reaction was negligible. The galactose concentration has remained typically below 1-3% w·w⁻¹.

These results provided a reference for the enzyme concentrations to be applied in subsequent GOS synthesis experiments using EMR. GOS yields obtained from STR (923-9230 U·kg⁻¹) will be later compared to GOS yields achieved in EMR (see Sect. 4.3 and Sect. 4.4). The results of STR will also be used as a calibration curve for quantifying enzyme loss during cyclic-EMR (Sect. 4.4.1).

4.3. Enzymatic conversion in continuous-EMR

4.3.1. Preliminary filtration experiments

Preliminary filtration tests were conducted to investigate the effects of reaction fluids and operating parameters on the filtration performance of ultrafiltration membranes during enzyme-catalyzed reactions. More specifically, the effects of transmembrane pressure, enzyme load, and operating time were determined in terms of membrane permeability, or rather, the permeate flux. The purpose of this study was to determine the set of design parameters of the EMR (such as the membrane area, the reactor volume, the residence time, and the trans-membrane pressure) that will ensure stable product flow levels over a long period of time.

4.3.2. Enzymatic conversion short-term

Examinations of the steady-state performance of the EMR in relation to enzyme loading and residence time was carried out in eight short-term (6-8 h) experiments. In each of the eight short-term experiments, reactions were performed using 2 kg of reaction fluid, and the permeate flow rate was set to a constant value by adjusting the permeate pump to control the reaction fluid flow rate. To adjust the required residence time for each experiment, different permeate flow rates varied from 0.9 to 1.9 kg·h⁻¹. An HPLC system was applied to measure the composition of the periodic samples as the experiment progressed to determine the carbohydrate concentration changes in the reaction solution. A brief summary of the composition of the steady-state carbohydrate during short-term runs can be found in Table 1.

Table 1. Steady-state saccharides' composition in w·w⁻¹% for short-term EMR runs. The composition obtained for batch process (at 6 h) was indicated for comparison purpose.

Component:	No3	No5	No2	No7	No4	No6	No1	No8	Batch
τ [h]	1.1	2.1	2.2	2.6	1.1	2.1	2.2	2.8	6.0
c_E [U·kg ⁻¹]	9230	8307	9230	9230	92301	83994	92301	92301	8307
$\tau \times c_E$ [U·h·kg ⁻¹]	10153	17279	20306	24090	104300	174708	205113	260289	49842
P [g·h ⁻¹ ·U ⁻¹] $\times 10^{-3}$	7.263	4.757	4.787	3.860	0.955	0.574	0.480	0.368	2.280
DP2	63.8	61.7	50.5	53.8	45.0	41.9	40.2	41.7	40.5
Glu	11.7	10.5	17.1	14.3	18.6	20.8	20.8	22.2	19.5
Gal	0.0	0.4	0.0	0.9	3.3	3.8	6.2	4.2	2.2
DP3	19.7	22.0	22.9	22.9	21.6	20.6	20.6	20.7	22.5
DP4	4.4	5.4	7.5	6.8	7.9	8.8	8.3	8.6	10.2
DP5	0.6	0.0	1.9	1.3	2.7	4.0	3.7	2.6	5.1
DP6	0.0	0.0	0.2	0.0	1.0	0.0	0.1	0.0	0.0
DP3-6	24.6	27.4	32.4	31.0	33.2	33.4	32.8	31.9	37.9

As indicated in Sect. 4.1.2, both enzyme dosages (c_E) and the residence time (τ) have certain effects on the synthesis of GOS. In order to explain and visualize the combined impacts of both factors, I employ the product of enzyme load and residence time ($\tau \times c_E$, in U·h·kg⁻¹) as a straightforward indicator of the applied settings that determine product quality. A gradual decline in productivity from approx. 7.263×10^{-3} to 0.368×10^{-3} g of DP3-6 per hour and unit enzyme activity has been observed when the value of $\tau \times c_E$ increased from 10153 to 260289 U·h·kg⁻¹.

Figure 4 illustrates the saccharides composition as function of $\tau \times c_E$.

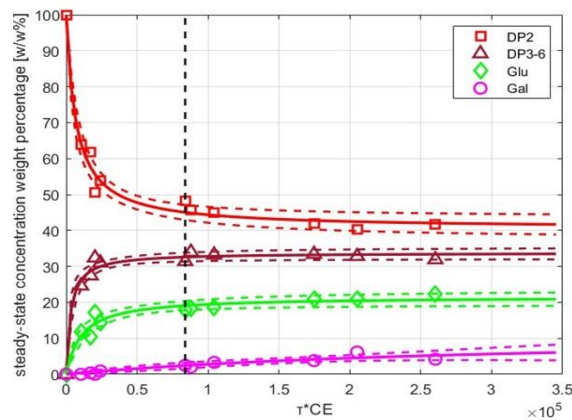


Figure 4. Steady-state composition saccharides as function of $\tau \times c_E$ for short-term runs. Experimental data fitted regression models, and simultaneous 95% confidence bounds were illustrated with symbols, solid lines, and dashed lines, respectively. Data obtained for long-term runs L1 and L2 at 8 h of operation was highlighted with a vertical line at $\tau \times c_E = 83070$ U·h·kg⁻¹.

In practice, I may set any values of τ and c_E , the factor $\tau \times c_E$ will determine the concentration of each component as dictated by the curves shown in Figure 4. Eq. 3.5.5-1 and Eq. 3.5.5-2 were fitted to the observed carbohydrate fraction concentrations. The interaction of residence time (τ) and enzyme load (c_E) were used as a predictor, and the relative mass percentage of the sugar fraction (w_i) was used as a response variable for the nonlinear regression. A diagram illustrating the model estimates and the simultaneous 95% confidence bounds was depicted in Figure 4.

As indicated in Figure 4, the DP3-6 fraction initially showed a trend of increasing in concentration with a higher value of $\tau \times c_E$ and gradually reached stability at $Y \approx 33\% \text{ w} \cdot \text{w}^{-1}$ after $\tau \times c_E = 100,000$. A continued increase in the content of $\tau \times c_E$ results in the formation of hydrolysis by-products. Furthermore, in comparison with the STR (38% $\text{w} \cdot \text{w}^{-1}$), the EMR DP3-6 yield (25-33% $\text{w} \cdot \text{w}^{-1}$) was lower. This result is consistent with findings of my in-silico study (see Sect. 4.1.2). More precisely, the predicted GOS yield in continuous-EMR is slightly lower than in STR (30% $\text{w} \cdot \text{w}^{-1}$ vs 34% $\text{w} \cdot \text{w}^{-1}$, respectively). In addition, the same trend was observed for the factor $\tau \times c_E$ on GOS yield. That is, GOS concentration increases with increasing $\tau \times c_E$ and reaches a maximum GOS concentration at a fixed value ($\tau \times c_E = 1.8 \times 10^5 \text{ U} \cdot \text{h} \cdot \text{kg}^{-1}$ in-silico vs $\tau \times c_E = 1.7 \times 10^5$ continuous-EMR), followed by a decline. The results indicate that the nonlinear model has an excellent predictive ability for the concentrations of DP2, DP3-6 (GOS), and glucose in solution at a steady state for different the factor $\tau \times c_E$. The model achieved an R^2 value exceeding 0.95 for both DP2, DP3-6 (GOS), and glucose.

4.3.3. *Enzymatic conversion in long-term*

The long-term experiments (runs L1 and L2) were conducted under the same operating conditions as the short-term experiments, i.e., 30% $\text{w} \cdot \text{w}^{-1}$ feed lactose, 30% $\text{w} \cdot \text{w}^{-1}$ initial lactose concentration, pH 6.0, and 50 °C. The EMR was run continuously for more than 120 hours in both runs, with an initial enzyme concentration of 46151 $\text{U} \cdot \text{kg}^{-1}$. The average amount of lactose used as feed was 40 kg (30% $\text{w} \cdot \text{w}^{-1}$ lactose solution), resulting in an output of 130 kg of liquid product per run. Since the feed enzyme in the EMR was approximately 10 g, for the entire campaign, an average of approx. 1.4 kg of DP3-6 was produced by one gram of crude enzyme preparation. Figure 5 illustrates the

composition of saccharides in the product stream as a function of operating time for Run L1 and Run L2.

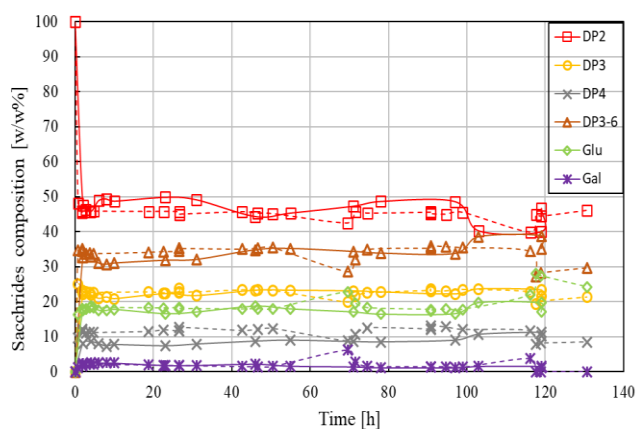


Figure 5. Saccharides composition in permeate as function of operational time in enzymatic membrane reactor for both Run L1 (solid line) and Run L2 (dashed line). Operational conditions: 30% w·w⁻¹ feed lactose concentration, 30% w·w⁻¹ initial lactose concentration, 46151 U·kg⁻¹ enzyme load, pH 6.0, 50 °C, ca. 1.8 h residence time, 0.16 m³·h⁻¹ crossflow rate, 1.0 bar retentate-side pressure, 0.7-0.2 bar permeate-side pressure, 10 kDa UF membrane.

These manipulations provide comparable results, more specifically, intercomparisons between long-term experiments and short-term manipulation results. The steady-state compositions obtained in the long-term runs (averages calculated from samples taken over a period of approximately 5-10 hours) were consistent with those obtained in the previous short-term runs (see the horizontal line in Figure 4). In long-term runs, the steady-state concentrate of DP2 in a range of 40-50% w·w⁻¹, and GOS yield between 30-40% w·w⁻¹. There was no significant membrane fouling was observed. In both short- and long-term investigations, more than 75% of the initial membrane permeability was restored after the membrane cleaning process, indicating that the membrane was successfully regenerated after the experiment. In most instances, water permeability ($\approx 18 \pm 3.6 \text{ kg} \cdot \text{h}^{-1} \cdot \text{m}^{-2}$) was restored by applying alkaline cleaning.

Based upon the comparison of long-term results with those of STR, the STR experiment was clearly superior to the EMR experiment, both in terms of yield (38% w·w⁻¹ vs. 33% w·w⁻¹) and biocatalyst productivity (2.280×10^{-3} vs. $1.180 \times 10^{-3} \text{ g} \cdot \text{h}^{-1} \cdot \text{U}^{-1}$). However, the amount of product (DP3-6) obtained per hour for one kg of reactor content was calculated as 54.5 g·kg⁻¹·h⁻¹ for the long-term runs which was significantly higher than the amount obtained with STR (18.9 g·kg⁻¹·h⁻¹).

¹). Additionally, under the studied operational conditions, the amount of DP3-6 produced by one gram of enzyme preparation was significantly greater in EMR (ca. 1.4 g·kg⁻¹) than in STR (ca. 0.13 g·kg⁻¹).

As reported in Figure 5, the stability of Biolacta N5 and the consistent degree of lactose conversion maintained throughout such an extended operational period was unexpected. In addition to what has been said previously, no reports have been published pertaining to the operational stability of Biolacta N5 in EMR. The $\tau \times c_E$ factor for the long-term run was adjusted to approximately 83911 U·h·kg⁻¹. In this setting, it is possible to gain a greater understanding of the mechanism of enzyme activity decline during a long-term EMR experiment. In this experiment, Biolacta N5 was expected to have a half-life of approximately 24 hours according to Warmerdam et al. (2013).

Starting a long run with an enzyme dosage of 46151 U·kg⁻¹ ($\tau \times c_E = 83070$ U·h·kg⁻¹) means that the concentration of active enzyme was expected to drop to 23075.5 U·kg⁻¹ ($\tau \times c_E = 41536$ U·h·kg⁻¹) after approximately one day of running. By the end of the experiment, at ca. 120 hours, $\tau \times c_E$ was expected to reach the value of 2596 U·h·kg⁻¹. Figure 4 reports the proven output of EMR for any given value of $\tau \times c_E$. Therefore, by following the expected decrease in $\tau \times c_E$ from our starting situation ($\tau \times c_E = 83070$ U·h·kg⁻¹) to $\tau \times c_E = 2596$ U·h·kg⁻¹, one can read the corresponding degree of conversion from the vertical axis in Figure 4. Presuming a half-life of 24 h, the regression models (Eq. 3.5.5-1 and Eq. 3.5.5-2) estimated a dramatic drop in product quality after 5 days of operation, resulting in a saccharide composition of $84.1 \pm 4.4\%$ w·w⁻¹ DP2, $15.5 \pm 5.2\%$ w·w⁻¹ DP3-6, and $4.2 \pm 2.0\%$ w·w⁻¹ glucose. However, despite prolonged EMR operation (within 120-130 h), no significant decrease in conversion was observed for each component of the reaction solution. This result differs from the predicted results in in-silico (Sect. 4.1.3) and the results of Warmerdam et al. (2013) that the half-life of Biolacta N5 at pH 6.0, 40°C is approx. 29h. In view of the stable performance of the EMR, HPLC data collected from L1 and L2 cannot be extrapolated to determine the true value of the half-life of the enzyme. It is therefore necessary to conduct additional experiments in order to determine the half-life of Biolacta N5. It is possible to extrapolate accurate half-life values through longer experiments at a reduced EMR scale.

4.4. Cyclic-EMR

4.4.1. Performance assessment in STR

The enzyme activity varies from 923 to 8307 U·kg⁻¹ for the five batches of experiments used for calibration purposes. In the presence of elevated enzyme activity (above 8307 U·kg⁻¹), the production of DP3-6 and the consumption of lactose were at an astounding rate, and galactose was produced at significant rates. These phenomena make the results of operations performed at these enzyme concentrations unsuitable for calibration.

Table 2. Estimated parameters for the saturation model (Eq. 4.4.2-1) for different enzyme activities (rounded for two digits), their standard errors and 95 % confidence intervals together with the model accuracy F-tests and the explained variance rates (R^2) and the initial reaction velocity values ($p_1 \times p_2$).

Enzyme activity (U·kg ⁻¹)	Parameters	Estimate	Std. Error	95% Confidence Interval		F (2; df ₂)	R^2	$p_1 \times p_2$ (g·kg ⁻¹ ·h ⁻¹)
				Lower Bound	Upper Bound			
923	p_1	-162.07*	3.11	155.30	168.84	28504.6* df ₂ =12	>0.99*	-22.69
	p_2	0.14*	0.01	0.13	0.15			
2307	p_1	-172.91*	2.92	166.56	179.27	5352.4* df ₂ =12	0.99*	-70.03
	p_2	0.41*	0.03	0.35	0.46			
4615	p_1	-180.19*	3.35	172.60	187.76	4539.8* df ₂ =9	0.99*	-134.24
	p_2	0.75*	0.06	0.62	0.87			
6923	p_1	-177.63*	1.64	174.07	181.20	6763.6* df ₂ =12	0.99*	-220.44
	p_2	1.24*	0.08	1.08	1.41			
8307	p_1	-179.05*	1.72	175.53	182.56	8630.4* df ₂ =29	0.99*	-237.95
	p_2	1.33*	0.07	1.20	1.46			

* Significant at $p < 0.001$

In all cases, the DP3-DP6 fraction increased gradually by the reaction time, then reached a plateau at $35.9 \pm 1.8\%$ w·w⁻¹ on total carbohydrate basis. The extent of hydrolysis activity, as measured by the amount of generated galactose, was negligible. The galactose concentration has remained typically below 1-3% w·w⁻¹. The saturation models (Eq. 3.4.2-1) were fitted to the observed concentration profiles. The results of curve fitting procedure, including the estimated parameters, their standard errors and 95 % confidence intervals together with the model accuracy F-tests, the explained variance rates (R^2) and the initial reaction velocity values ($p_1 \times p_2$) were summarized in Table 2. In general, the observed data were consistent with the models that were assumed.

Each saccharide fraction was subjected to a determination of the initial reaction rate ($p_1 \times p_2$). This value will be subsequently used as a measure of enzyme activity. According to the results, linear models fit well with the observed data for all saccharide fractions within the investigated range of enzyme load (from 923 to 8307 U·kg⁻¹). All the linear models and their parameters were proven to be significant ($p < 0.001$). By integrating the reaction rate data in the experiment with the slopes of the linear models listed in Table 3 which can be used for calibration purposes. The amount of unknown enzyme loading can be calculated from the progress curve.

Table 3. The slopes of the no-intercept linear regression functions fitted to the reaction velocity (Y) depending on enzyme activity for different saccharides fractions.

Saccharides compounds	no-intercept linear regression slopes	R ²
DP2	0.03 *	0.997 *
DP3	0.025 *	0.991 *
DP4	0.004 *	0.995 *
DP3-6	0.024 *	0.997 *
Glucose	0.007 *	0.999 *

* Significant at $p < 0.001$

4.4.2. Enzymatic conversion in cyclic-EMR

The cyclic EMR system consists of a stirred tank reactor and an external ultrafiltration module. Under the prescribed conditions, the GOS generation process was carried out in five consecutive cycles. A progression curve for each saccharide over five consecutive cycles was investigated. Each reaction step was conducted under the same reaction conditions, pH 6.0 and 50°C, for a period of about 24 hours. The initial lactose concentration and initial enzyme activity were set at 300 g·kg⁻¹ and 8307 U·kg⁻¹, respectively. Modeling of experimental data was conducted using the saturation model described in Sect. 3.4.2. Specifically, initial reaction rates ($p_1 \times p_2$) for each saccharides' fraction were determined by estimating the parameters p_1 and p_2 .

Following the lactose conversion reaction in STR, the complete reaction mixture was transported to the ultrafiltration procedure. The reaction solution was concentrated by a volume concentration factor of 8.6. Upon completion, the reaction solution was filtered in order to collect the GOS product from the permeate and to recover the enzyme from the concentrate, enabling the reaction step to be repeated.

4.4.3. Quantification of enzyme losses

It is clear from the results that there has been a progressive decline in the rate at which GOS was synthesized, and lactose was converted from cycle 1 to cycle 5. A loss of enzyme activity was believed to be responsible for the observed decreases. To quantify these losses, I first determined the initial reaction rates of the individual saccharides by fitting the obtained experimental data to the progression curves through a saturation model. Following previous STR experiments using known enzyme concentrations (Table 3), linear models were used to calculate the respective enzyme activity values for each cycle. These models were used as calibration curves to determine the unknown (residual) enzyme activity values for successive cycles.

In Table 4, residual enzyme activity values were presented for DP2, DP3, DP3-6, and glucose in the reaction solution for five consecutive cycles. According to the results, the activity values obtained were independent of the type of saccharides used in the estimation process. In other words, all listed components return with close approximations of the remaining activity. Table 4 indicates that enzyme activity decreases with each cycle.

Table 4. Enzyme activity values [$\text{U} \cdot \text{kg}^{-1}$] for the 5 consecutive cycles as determined by analyzing the reaction rates of different saccharides fractions.

Fractions	Cycles				
	No.1	No.2	No.3	No.4	No.5
DP2	7077	2124	846	388	329
DP3	7925	2480	890	379	306
DP3-6	6999	2081	785	355	295
Glucose	7903	2588	992	448	400
Mean	7476	2318	878	392	333
STDEV	507	254	87	40	47

The various enzyme deactivation models (Eq. 3.3-8 - Eq. 3.3-12) mentioned previously in Sect. 3.3. with respect to enzymes were fitted globally to all available data points by introducing non-negative constraints on the model parameters. Table 5 summarizes the results of parameter estimation. In general, favorable overall fittings were achieved for all implemented models. It should be noted that the first-order deactivation model (Eq. 3.3-12) tends to underestimate activity in the last phases of the investigation period, i.e., for lower activity values. The goodness of fit was

not significantly different between the single-stage model with a non-zero final stage (Eq. 3.3-11), and the more complex two-stage models (Eq. 3.3-8 and Eq. 3.3-9) with 3 and 4 fitting parameters, respectively.

It is noted that the half-life of 15.3 h achieved in this study was in reasonable agreement with the results reported by (Warmerdam et al., 2013) using similar operational settings. In their prior investigation, the half-life of Biolacta N5 at an initial lactose content of $300 \text{ g}\cdot\text{L}^{-1}$ was determined to be 29 hours, 29 hours, and 16 hours, respectively, at temperatures of 20, 40, and 60 °C.

Table 5. Estimated parameters of the inactivation models (Eq. 3.3-8 - Eq. 3.3-12).

Model	k₁	k₂	α₁	α₂	R²	SSR
Eq. 3.3-8	9.692×10^{-1}	4.839×10^{-2}	8.125×10^{-1}	2.977×10^{-2}	0.9974	7.338×10^{-3}
Eq. 3.3-9	5.947×10^{-2}	9.980×10^{-3}	7.493×10^{-2}	0	0.9987	3.535×10^{-3}
Eq. 3.3-11	5.537×10^{-2}	0	3.651×10^{-2}	0	0.9986	3.674×10^{-3}
Eq. 3.3-12	4.891×10^{-2}	0	0	0	0.9957	1.194×10^{-2}

It is worth noting that modeling the observed enzyme activity data using Eq. 3.3-8 - Eq. 3.3-12 was performed under the assumption that the reactions were performed under stable operating conditions. Under the assumed conditions, the activity of the enzyme decreases continuously and gradually during the reaction. However, in my study, a series of repeated reactions and filtration steps were performed. In the filtration step, the enzymes were recirculated by the retention of the membrane assembly and concentrated in the retentate. Therefore, there were some limitations associated with the model developed. Retained enzymes accumulate on the membrane surface during crossflow filtration, forming a concentration polarization layer that may enhance fouling and partially inactivate biocatalysts (Córdova et al., 2016a). The methods used for this study do not allow to quantify the extent of the activity decline caused by the filtration procedure and its relation to the stability in STR during the reaction steps. Despite the fact that this fact suggests that the filtration steps do not affect enzyme stability to a pronounced extent, further investigation was required to determine the separate effects of the reaction and the filtration procedure on enzyme stability.

5. CONCLUSION AND RECOMMENDATIONS

Galacto-oligosaccharides (GOS) are indigestible oligosaccharides with prebiotic effects and are widely used as an additive in infant formulas, dairy products, and beverages. Commercially, GOS were produced primarily through catalytic reactions in stirred tank reactors (STR) using soluble β -galactosidase. However, one significant limitation of this conventional method were the high operational costs, which related to the non-reusability of the enzyme. Ultrafiltration membrane-assisted enzyme membrane reactors have been reported to have the ability to achieve enzyme reuse. However, the performance of Biolacta N5, a commercial enzyme preparation derived from *Bacillus circulans* in generating GOS in EMR has not been studied.

In my Ph.D. research, I evaluated the potential of using soluble Biolacta N5 for GOS production in continuous-EMR and cyclic-EMR, respectively. An extended mathematical model was successfully applied to simulate the performance of continuous-EMR for the synthesis of GOS. In other words, the changes in the individual saccharide fractions over time. Different residence times and enzyme activities were found to have effects on GOS yield, and it was found that the maximum GOS yield at steady-state (approx. 30% w·w⁻¹) was obtained at $\tau \times c_E$ of $2 \times 10^5 \text{ U} \cdot \text{h} \cdot \text{kg}^{-1}$ within the studied range. Simulation experiments considering enzyme inactivation in continuous-EMR obtained an enzyme half-life of ca. 29h. The simulation results demonstrated that in the actual continuous-EMR process, timely replenishment of fresh enzymes is necessary to ensure consistent quality.

I performed a series of short and long experiments to investigate the operational stability of Biolacta N5 in continuous-EMR. The results observed for the effect of different residence times and enzyme concentrations on GOS production showed a similar tendency as in the previous simulations. When controlling the operating factor ($\tau \times c_E$) from $10^4 \text{ U} \cdot \text{h} \cdot \text{kg}^{-1}$ to $2.6 \times 10^5 \text{ U} \cdot \text{h} \cdot \text{kg}^{-1}$, the GOS yield increased from 24% w·w⁻¹ to 33% w·w⁻¹. However, GOS productivity decreased from approximately 7×10^{-3} to $0.4 \times 10^{-3} \text{ g} \cdot \text{h}^{-1} \cdot \text{U}^{-1}$. The maximum GOS yield of 33% w·w⁻¹ obtained at steady-state in the continuous-EMR experiments was slightly lower than that in the STR under the same conditions (~38% w·w⁻¹). This phenomenon in agreement with the results of the previous

simulation experiments, i.e., lower yield in continuous-EMR. A stable catalytic performance without a significant deterioration in product quality was observed when operating the EMR for an extended period of time (>120 h). Approx. 1.4 kg of DP3-6 was produced per one gram of crude enzyme preparation over the long-term campaigns, indicating that EMR efficiently recovers enzyme activity (stability).

In cyclic-EMR, GOS synthesis was performed in a batchwise manner in five consecutive cycles. A volume concentration factor of 8.6 was achieved to successfully separate the carbohydrates from the enzyme using an ultrafiltration module. The collected enzymes were used in the next cycle to catalyze the conversion of fresh lactose. Enzyme losses during consecutive cycles was successfully quantified with a direct approach by analyzing the underlying relationship between reaction rate and enzyme dosage obtained from additional experiments with known enzyme loads. Within five cycles, the enzyme activity declined gradually from 7476 to 333 U·kg⁻¹, and the half-life was estimated as ca. 15.3 h.

All these results suggest that EMR might serve as a promising alternative to conventional batch production scheme, especially considering the high price of the biocatalysts. In addition, the outcomes of my research may serve as a basis for further optimization GOS production in EMR.

6. NEW SCIENTIFIC RESULTS

Within the frame of this work, I investigated the technical feasibility of galacto-oligosaccharides (GOS) production by ultrafiltration (UF)-assisted enzyme membrane reactors (EMR) operating in both continuous and cyclic fashion using free enzymes Biolacta N5 originating from *Bacillus circulans*. My new scientific achievements can be summarized as:

- 1) I have developed an extended mathematical framework to predict the production of GOS in continuous-EMRs by free β -galactosidases. By simulating the dynamics of formulation of saccharides in continuous-EMR for various residence times (0-10 h) and enzyme load of Biolacta N5 (0-10 g·kg⁻¹), my in-silico study suggests that continuous-EMR underperforms STR in the term of steady-state GOS yield (30% w·w⁻¹ vs. 34% w·w⁻¹ for continuous-EMR and STR, respectively) under the same operational conditions (320 g·kg⁻¹ lactose solution, pH 6.0, and 40°C).
- 2) By using soluble Biolacta N5, a *Bacillus circulans*-derived commercial enzyme preparation, I have experimentally investigated the steady-state performance of the continuous-EMR as function of residence time (1.1-2.8 h) and enzyme load (8307-92301 U·kg⁻¹) under fixed operational settings (50°C, pH 6.0, lactose feed concentration of 300 g·kg⁻¹, and recirculation flowrate of 0.18 m³·h⁻¹). My results indicate that the yield increased from 24% w·w⁻¹ to 33% w·w⁻¹, whereas the productivity decreased from ca. 7×10^{-3} to 0.4×10^{-3} g·h⁻¹·U⁻¹, when adjusting $\tau \times C_E$, from 10153 to 260289 U·h·kg⁻¹. I also found that the yield of oligosaccharides with higher degree of polymerization (DP3-6) in STR (approx. 38% on total carbohydrate basis) slightly exceeds that measured in continuous-EMR (ranging from 24% w·w⁻¹ to 33% w·w⁻¹). This finding is in good agreement with my preliminary simulation results, as in reported above in 1).
- 3) A stable catalytic performance without a significant deterioration in product quality was observed when operating the continuous-EMR for an extended period of time (>120 h). Under the investigated operational settings (46151 U·kg⁻¹ Biolacta N5, 30% w·w⁻¹ lactose solution, pH 6.0, 50°C, 0.16 m³·h⁻¹ recirculation flowrate, and residence time of 1.8h), approx. 1.4 kg

of DP3-6 was produced per one gram of crude enzyme preparation over the long-term campaigns. I proved that the operational stability of the enzyme in continuous-EMR is considerably higher than previously reported for STR in the literature (Warmerdam et al., 2013).

- 4) I proposed a process scheme for enzyme recovery by operating the EMR in cyclic fashion. Repeated reaction steps ($8307 \text{ U} \cdot \text{kg}^{-1}$ initial Biolacta N5, 30% w·w⁻¹ lactose solution, pH 6.0, 50°C) were performed and followed by UF steps employing a volume concentration factor of 8.6 to separate the carbohydrate products from enzymes. I quantified the enzyme losses with a direct method by analyzing the underlying relationship between reaction rates and enzyme dosage obtained from additional experiments conducted with known enzyme loads. I found that the enzyme activity in the cyclic-EMR declined gradually from $8307 \text{ U} \cdot \text{kg}^{-1}$ to $923 \text{ U} \cdot \text{kg}^{-1}$ within five cycles, resulting in a half-life of approx. 15.3 h. The resulting half-life is comparable to those previously reported by Warmerdam et al. (2013) in STR.

7. PUBLICATIONS

1. Articles in a magazine/journal:

Cao, T., Pázmándi, M., Galambos, I. and Kovács, Z., 2020. Continuous production of galacto-oligosaccharides by an enzyme membrane reactor utilizing free enzymes. *Membranes*, 10(9), p.203. <https://doi.org/10.3390/membranes10090203> (***Membranes*, Impact Factor: 4.13 (2020), JCR – Q2 (Chemical Engineering).**

Cao, T., Kovács, Z. and Ladányi, M., 2023. Cyclic Production of Galacto-Oligosaccharides through Ultrafiltration-Assisted Enzyme Recovery. *Processes*, 11(1), p.225. <https://doi.org/10.3390/pr11010225> (***Processes*, Impact Factor: 3.352, JCR - Q2 (Engineering, Chemical)).**

2. Abstracts in conferences

Teng, C. et al., 2021. Ultrafiltration-based enzyme recovery in the batch production of galacto-oligosaccharides. *In 4th International Conference on Biosystems and Food Engineering. Budapest, Hungary, 4th June, 2021.* <http://www.biosysfoodeng.hu/2021/USB/#proceedings>

Teng, C. et al., 2021. The continuous production and real-time monitoring of galacto-oligosaccharides. *In 9th European Young Engineers Conference. Warsaw, Poland, 19–21 April 2021.* pp. 150. https://www.eyec.ichip.pw.edu.pl/wp-content/uploads/Monografia_EYEC_9th.pdf

Teng, C. et al., 2019. Method for Real-time Monitoring of Galactooligosaccharides Production by Means of Fourier Transform Near-Infrared Spectroscopy. *In Second Aquaphotomics European Conference. Budapest, Hungary, 2-3 December 2019.* pp. 28–28.

8. REFERENCES

- ALBAYRAK, N. & YANG, S. T. 2002. Production of galacto-oligosaccharides from lactose by *Aspergillus oryzae* β -galactosidase immobilized on cotton cloth. *Biotechnology and Bioengineering*, 77, 8-19.
- CHEN, X. Y. & GÄNZLE, M. G. 2017. Lactose and lactose-derived oligosaccharides: More than prebiotics? *International Dairy Journal*, 67, 61-72.
- CÓRDOVA, A., ASTUDILLO, C., GIORNO, L., GUERRERO, C., CONIDI, C., ILLANES, A. & CASSANO, A. 2016a. Nanofiltration potential for the purification of highly concentrated enzymatically produced oligosaccharides. *Food and Bioproducts Processing*, 98, 50-61.
- CÓRDOVA, A., ASTUDILLO, C., VERA, C., GUERRERO, C. & ILLANES, A. 2016b. Performance of an ultrafiltration membrane bioreactor (UF-MBR) as a processing strategy for the synthesis of galacto-oligosaccharides at high substrate concentrations. *Journal of Biotechnology*, 223, 26-35.
- DAS, R., SEN, D., SARKAR, A., BHATTACHARYYA, S. & BHATTACHARJEE, C. 2011. A comparative study on the production of galacto-oligosaccharide from whey permeate in recycle membrane reactor and in enzymatic batch reactor. *Industrial & Engineering Chemistry Research*, 50, 806-816.
- DE ALBUQUERQUE, T. L., DE SOUSA, M., E SILVA, N. C. G., NETO, C. A. C. G., GONÇALVES, L. R. B., FERNANDEZ-LAFUENTE, R. & ROCHA, M. V. P. 2021. β -Galactosidase from *Kluyveromyces lactis*: Characterization, production, immobilization and applications-A review. *International Journal of Biological Macromolecules*, 191, 881-898.
- FIJAN, S. 2014. Microorganisms with claimed probiotic properties: an overview of recent literature. *International Journal of Environmental Research and Public Health*, 11, 4745-4767.
- GÄNZLE, M. G. 2012. Enzymatic synthesis of galacto-oligosaccharides and other lactose derivatives (hetero-oligosaccharides) from lactose. *International Dairy Journal*, 22, 116-122.
- HUANG, J., ZHU, S., ZHAO, L., CHEN, L., DU, M., ZHANG, C. & YANG, S.-T. 2020. A novel β -galactosidase from *Klebsiella oxytoca* ZJUH1705 for efficient production of galacto-oligosaccharides from lactose. *Applied Microbiology and Biotechnology*, 104, 6161-6172.
- IBM CORP. RELEASED 2017. IBM SPSS STATISTICS FOR WINDOWS, V. A., NY: IBM CORP.
- KERRY, R. G., PATRA, J. K., GOUDA, S., PARK, Y., SHIN, H.-S. & DAS, G. 2018. Benefaction of probiotics for human health: A review. *Journal of Food and Drug Analysis*, 26, 927-939.
- MATELLA, N., DOLAN, K. & LEE, Y. 2006. Comparison of galactooligosaccharide production in free-enzyme ultrafiltration and in immobilized-enzyme systems. *Journal of Food Science*, 71, C363-C368.
- MATLAB R2015a. MATLAB. R2015a ed. Natick, MA: MathWorks.
- PALAI, T., MITRA, S. & BHATTACHARYA, P. K. 2012. Kinetics and design relation for enzymatic conversion of lactose into galacto-oligosaccharides using commercial grade β -galactosidase.

- Journal of Bioscience and Bioengineering*, 114, 418-423.
- PARK, A.-R. & OH, D.-K. 2010. Galacto-oligosaccharide production using microbial β -galactosidase: current state and perspectives. *Applied Microbiology and Biotechnology*, 85, 1279-1286.
- PÁZMÁNDI, M., MARÁZ, A., LADÁNYI, M. & KOVÁCS, Z. 2018. The impact of membrane pretreatment on the enzymatic production of whey-derived galacto-oligosaccharides. *Journal of Food Process Engineering*, 41, e12649.
- PETZELBAUER, I., SPLECHTNA, B. & NIDETZKY, B. 2002. Development of an ultrahigh-temperature process for the enzymatic hydrolysis of lactose. III. Utilization of two thermostable β -glycosidases in a continuous ultrafiltration membrane reactor and galacto-oligosaccharide formation under steady-state conditions. *Biotechnology and Bioengineering*, 77, 394-404.
- POCEDIČOVÁ, K., ČURDA, L., MIŠÚN, D., DRYÁKOVÁ, A. & DIBLÍKOVÁ, L. 2010. Preparation of galacto-oligosaccharides using membrane reactor. *Journal of Food Engineering*, 99, 479-484.
- REN, H., FEI, J., SHI, X., ZHAO, T., CHENG, H., ZHAO, N., CHEN, Y. & YING, H. 2015. Continuous ultrafiltration membrane reactor coupled with nanofiltration for the enzymatic synthesis and purification of galactosyl-oligosaccharides. *Separation and Purification Technology*, 144, 70-79.
- SCOTT, F., VERA, C. & CONEJEROS, R. 2016. Technical and economic analysis of industrial production of lactose-derived prebiotics with focus on galacto-oligosaccharides. *Lactose-derived prebiotics: A process perspective*. Elsevier Inc.
- TORRES, D. P., GONÇALVES, M. D. P. F., TEIXEIRA, J. A. & RODRIGUES, L. R. 2010. Galacto-oligosaccharides: production, properties, applications, and significance as prebiotics. *Comprehensive Reviews in Food Science and Food Safety*, 9, 438-454.
- TORRES, P. & BATISTA-VIERA, F. 2012. Improved biocatalysts based on *Bacillus circulans* β -galactosidase immobilized onto epoxy-activated acrylic supports: Applications in whey processing. *Journal of Molecular Catalysis B: Enzymatic*, 83, 57-64.
- URRUTIA, P., MATEO, C., GUIŠÁN, J. M., WILSON, L. & ILLANES, A. 2013. Immobilization of *Bacillus circulans* β -galactosidase and its application in the synthesis of galacto-oligosaccharides under repeated-batch operation. *Biochemical engineering journal*, 77, 41-48.
- VERA, C., GUERRERO, C., ILLANES, A. & CONEJEROS, R. 2011. A pseudo steady-state model for galacto-oligosaccharides synthesis with β -galactosidase from *Aspergillus oryzae*. *Biotechnology and Bioengineering*, 108, 2270-2279.
- WAN, M. L. Y., FORSYTHE, S. J. & EL-NEZAMI, H. 2019. Probiotics interaction with foodborne pathogens: a potential alternative to antibiotics and future challenges. *Critical Reviews in Food Science Nutrition*, 59, 3320-3333.
- WARMERDAM, A., BOOM, R. M. & JANSSEN, A. E. 2013. β -galactosidase stability at high substrate concentrations. *SpringerPlus*, 2, 1-8.

- WARMERDAM, A., ZISOPOULOS, F. K., BOOM, R. M. & JANSSEN, A. E. 2014. Kinetic characterization of galacto-oligosaccharide (GOS) synthesis by three commercially important β -galactosidases. *Biotechnology Progress*, 30, 38-47.
- WILSON, B. & WHELAN, K. 2017. Prebiotic inulin-type fructans and galacto-oligosaccharides: definition, specificity, function, and application in gastrointestinal disorders. *Journal of Gastroenterology and Hepatology*, 32, 64-68.